4 K, ultrahigh vacuum scanning tunneling microscope having two orthogonal tips with tunnel junctions as close as a few nanometers

J. F. Xu and P. M. Thibado
Department of Physics, University of Arkansas, Fayetteville, Arkansas 72701

Z. Ding
Department of Electronics, Guizhou University, Guiyang, Guizhou 550025, China

(Received 9 June 2006; accepted 8 August 2006; published online 25 September 2006)

An instrument that incorporates two scanning tunneling microscope (STM) tips which can have their tunnel junctions as close together as a few nanometers was designed and built. The sample is fixed and can be imaged simultaneously and independently with both STM tips. The tips and sample can be positioned and angled to image the same surface or perpendicular surfaces. The entire STM head is cooled with liquid helium to about 4 K while in an ultrahigh vacuum environment. Macroscopic positioning of the tips is accomplished using piezoelectric "stick-slip" coarse motion stages, whereas atomic positioning is accomplished with piezoelectric tube scanners. This instrument addresses the critical need to locally characterize individual nanostructures and heterostructures. © *2006 American Institute of Physics.* [DOI: 10.1063/1.2349599]

I. INTRODUCTION

Interest in developing next-generation nanoscale devices is at an all time high. New methods for fabricating nanostructures are being developed at an increasing rate. This includes novel self-assemble, artificially fabricated, lithography-etching techniques, etc. What has not kept pace is the number of new ways to characterize materials on these smaller scales. Consequently, the majority of characterization studies still average over a large volume or surface area containing numerous nanostructures. This method of characterization yields a signal that is inhomogeneously broadened from the desired result. At present, there is a critical need to add new techniques which precisely characterize individual nanostructures.

Lithographic techniques do allow for limited nanoscale characterization. One can pattern small windows using a shadow mask to perform optical measurements through the small window. In addition, one can pattern small electrical contacts and study carrier transport between the contacts. In fact, these methods have been the driving force behind numerous basic research studies as well as many technological breakthroughs.[1] For example, researchers have "tagged" electrons by giving them a certain magnetic moment orientation at one ferromagnetic metal lithographic injection point and then detected the tagged particles at another lithographic point in the material. This has led to the measurement of the spin-relaxation time T_2 for conduction electrons.[2]

There are several shortcomings when using lithographic techniques, however. First the patterning permanently alters your sample. Worse still, the structure and chemistry of the contacts and interface layers may unknowingly alter the experiment. Second, the contacts cannot be moved to a new location. In other words, one would ideally like these contacts to be mobile and nondestructive.

One of the best instruments for nondestructive probing is the scanning tunneling microscope (STM).[3–5] When used in combination with a scanning electron microscopy (SEM), these two imaging methods nicely bridge the gap from microns to nanometers.[6] If the STM is attached to a semiconductor fabrication chamber then one can study the interior structure of semiconductor devices by interrupting the fabrication process.[7–11] This has led to significant advancements in our understanding of technologically important surfaces.[12,13] Even still, these approaches are limited because the STM has only one local probe to inject or detect charge.

To address this need a handful of researchers have developed STM's which have two tips. One of the first designs of this type used two tips on a single scanner assembly.[14] This provides movable, nondestructive contacts where one can inject charge at a single point and detect it at another. Later, even better designs came along where both STM tips were mounted on their own scanner assembly.[15–18] This way each tip could independently image the surface and move to a desired location for charge injection and detection. This method has evolved considerably,[19] and now a four-probe STM is commercially available; however, it is designed for four-probe transport measurements and does not achieve atomic resolution.[20]

The main challenge remaining with all existing multiprobe STM designs is to find a way to get the two STM tip's tunneling junctions closer together, and more importantly know the relative distance between the two tunnel junctions. One would like this distance to be at least the same as the size of the nanostructure, and even better to be several times smaller than the nanostructure so as to be able to probe the nanostructure itself. The difficulty lies in the radius of each tip and the angle the tips approach the surface. If the tips get too close to each other, the tunnel junction between the tip and sample suddenly jumps from the sample to the second tip. This is called side tunneling. Also, if the tip approaches

 © 2006 American Institute of Physics

the surface at an angle that is not perpendicular then, it is unclear where the tunnel junction is located. Even the best tips have a main shaft diameter of several hundred nanometers near the end of the tip,[21] making this a significant technological problem.

We have built a system which overcomes these limitations with a flexible, clever design. This system has two STM tips that can be independently positioned on the same surface or perpendicular surfaces of the same sample. In addition, we can approach each surface at any angle we desire from perpendicular to off axis by 60° or more. Using two optical cameras with zoom magnification, we can watch both tips approach the corner of a sample. We can position the two tips within a few microns of each other. Then, by imaging with the two tube scanners we can have the two tips find the edge of the sample and then find each other. Once they are within nanometers of each other, we can study the transport properties of individual nanostructures that are in between the two tips. This design can be used in many subfields of surface science as well as characterizing the local transport properties through device structures.

One exciting example of a research area needing local characterization is called spintronics. This research area adds the spin degree of freedom to conventional charge-based electronics and offers opportunities for a new generation of devices. Our plans are to use one STM tip to inject spin-polarized carriers by using a ferromagnetic STM tip. These spin-polarized electrons will then travel to the other STM tip by going through some small section of the sample. This idea is similar to the lithography-based study mentioned earlier, except here we would have nondestructive, moveable point contacts. Ideally the sample would be a thin film heterostructure grown on a GaAs substrate. If the spin undergoes a spin-flip scattering event before reaching the second tip then the current flow will be modified. We will detect this modification in either the *I-V* characteristics of the second tip or in the topography characteristics.[22]

Furthermore, if the two tunnel junctions are close enough together, then the electrons can coherently move from one tunnel junction to the other even if the spins are not polarized. Similar to a resonant tunneling diode, by studying the *I-V* characteristics one can perform some basic fundamental studies of coupled tunnel junctions.[23]

II. INSTRUMENTATION

Our two-tip system consists of one UHV chamber, a low-temperature (LT) STM (4 K) head with two independently controlled tips, *in situ* sample and tip transfer capability, a manipulator with a sample heating/cleaving stage, electron-beam tip cleaning, load lock, two computers for data acquisition and control, and two sets of feedback electronics. The basic physical parameters of the two tips are shown in Table I. This includes signal-to-noise data and drift characteristics as well as scanning and vibration isolation properties. The current rms noise level of both tips was measured by collecting an image with a scan size of $100 \times 100\ \text{nm}^2$. After collecting the 400×400 data point image, we could build a height histogram. The width of the peak in the height histogram for the second tip scanner is about 0.1 nA for a current image and about 0.1 nm for a topography image. Note that our entire chamber is resting on a pneumatic controlled vibration isolation system. When the entire chamber is floating we can lock the sample stage to the main chamber (eliminating the spring suspension and eddy current dampening) and still obtain STM images with both the first tip and second tip.

TABLE I. Comparison of specifications for the scan size, coarse motion, drift, and noise [root mean square (rms)] for the first and second tips.

		First tip scanner/ coarse motion	Second tip scanner/ coarse motion
Maximum scan size	300 K	$10 \times 10\ \mu\text{m}^2$	$10 \times 10\ \mu\text{m}^2$
	77 K	$4.4 \times 4.4\ \mu\text{m}^2$	$4.4 \times 4.4\ \mu\text{m}^2$
	5 K	$1.8 \times 1.8\ \mu\text{m}^2$	$1.8 \times 1.8\ \mu\text{m}^2$
Coarse motion length (Z)		10 mm	10 mm
Scan drift		<1 nm/min	<1 nm/min
Vertical position (Z) noise (rms) while tunneling		0.05 nm	0.10 nm
Current (I) noise (rms) while tunneling		0.02 nA	0.10 nA
Vertical position (Z) noise (rms) without tunneling		0.004 nm	0.014 nm
Current (I) noise (rms) without tunneling		0.001 nA	0.002 nA

A. UHV chamber layout

At its core, the system utilizes a commercially available UHV LT-STM system (Omicron). The chamber is capable of operating in the low 10^{-10} Torr range via a 300 l/s ion pump. The entire chamber is mounted on a pneumatic vibration isolation system. In order to expand the functionality we also purchased a second coarse z-motion stage, a second tube scanner, a second set of electronics (with cables), a second computer, tee flanges for all the standard STM electrical feedthroughs, a second set of electrical feedthroughs, a linear motion feedthrough, and an alignment gimbals. The custom work includes a relatively small number of permanent modifications to the standard LT-STM. This way one could dismantle the two-tip system and recover the original system as needed. Specifically, we point out that surrounding the STM head are three cylindrical cups made of copper. These cups have some holes cut through them to allow the sample and tip transfer, but they also rotate to cover the holes when cooling to 4 K. We removed the two outer cups and machined a new hole through the inner cup for the second STM scanner assembly to pass through. Due to this modification the sample temperature will likely not reach 4 K, but we believe it should reach 20 K similar to the commercial variable-temperature (VT) STM design (Omicron). Extra electrical wires were also run from the new electrical feedthroughs to new jumper boards added below the inner cup. The electrical wires for the second STM tip connect to this jumper board. As a result of the way this system is designed, assembling the two-tip STM system must be done in sequence. First, we lower the standard STM head (approximately 1 m long) through the top 12 in. flange (using a

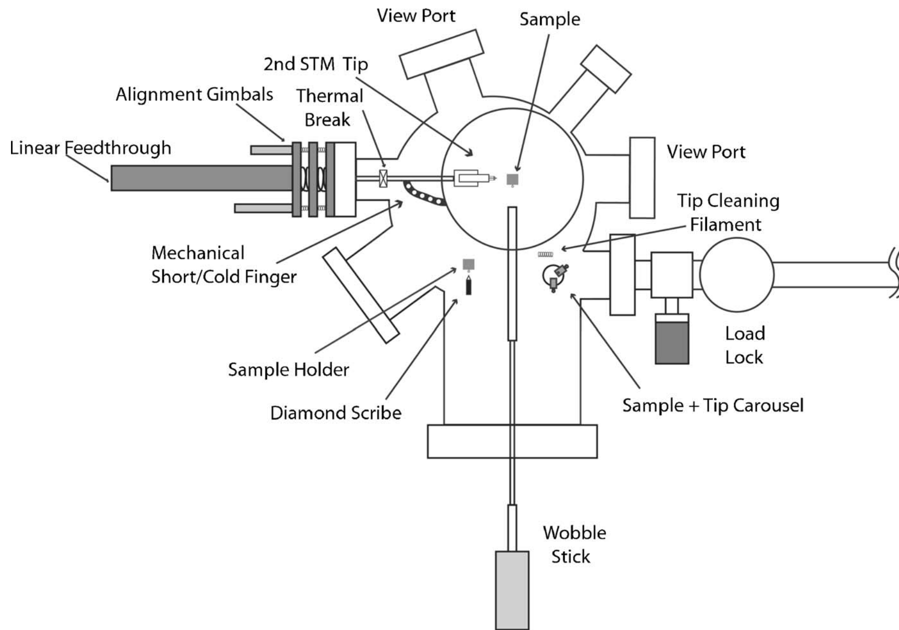

FIG. 1. Schematic diagram of the UHV chamber for the two-tip low-temperature STM system. This top view of the chamber shows the relative position of the equipment including the STM sample (first tip is below the sample and not shown), the second STM tip, the wobble stick, and the load lock.

ceiling crane), next we mount the second STM tip through the side port and pass it through the hole in the inner cup, and finally we connect the electrical wires between the jumper boards on the main STM head and the second STM tip. Once this is done the system can be pumped down and baked.

To show how all of these pieces fit together, a schematic top-view diagram of the central cylindrical chamber and load-lock area is shown in Fig. 1. As already mentioned, the UHV-STM with one STM tip (i.e., first STM tip) is mounted through a 12 in. flange at the very top of the chamber and it contains four $2\frac{3}{4}$ in. ports for electrical feedthroughs (note that the first tip is under the sample plate in this view and is not shown). The second STM tip is side mounted (see left side of Fig. 1) on a linear feedthrough combined with an alignment gimbals. In order to cool the second tip and stabilize it, a flexible metal bracket is bolted to the inner cup and pressed against the second scanner. In addition, a thermal break is positioned along the main axis of the linear transfer arm to help reduce heat flow from the outside. A wobble stick is also side mounted onto the main chamber (see bottom side of Fig. 1) and is used for sample and tip transfers. To add precision control to the wobble stick we have attached it to a three-axis micrometer stage. The micrometer is bolted to a hinged plate mounted to the outside of the chamber. Once the wobble stick is within a centimeter of its final transfer position it is clamped to the three-axis micrometer for the remaining part of the transfer. This helps when removing the second STM tip from the end of its tube scanner. The tip is removed when the scanner is fully retracted from the STM head using the linear motion feedthrough. A manipulator (not shown) is mounted on the 8 in. port just below the wobble stick, and contains several mini flanges used for mechanical supports for the sample heating and cleaving, as well as electrical connections and mechanical supports for electron-beam tip cleaning. A magnetically coupled linear-rotary feedthrough with 12 in. of linear movement, 360″ rotation, and a fork end that extends through the load-lock chamber is also side mounted (see right side of Fig. 1). This feedthrough is used to transfer the sample and tip between the carousel and the load-lock chamber, and is a standard product.

To summarize the chamber design section, a typical use of the chamber would entail the following. First, a sample and two tips enter the chamber through the load lock on the transfer fork. The sample would be mounted on the carousel and transferred with the wobble stick to the manipulator. Here the sample is heated to eliminate contaminants, scribed, and cleaved on two perpendicular surfaces, after which the sample would be transferred to the STM where it would be imaged. The tips are also originally mounted on the carousel and then transferred with the wobble stick to the electron-beam tip cleaning station. After heating to remove the oxide layer the tips are transferred to either tube scanner using the wobble stick.

B. Two-tip STM design

Five close-up photographs of the two-tip STM system are shown in Fig. 2. A photograph showing the main section of the STM chamber is shown in Fig. 2(a). In this photograph one can see the linear feedthrough that holds the second STM tip (left side) as well as the ports that holds the wobble stick and manipulator (items removed for camera shot). A close-up photograph showing the arm that holds second STM tip entering the inner cup is shown in Fig. 2(b). To the left one can see the support structure and to the right one can see the hole cut through the inner cup. A universal joint can be seen in this photograph. At one end, the universal joint attaches to the stainless steel rod that is directly attached to the linear feedthrough, while the other end holds a custom mount that is attached to the coarse motion stage. A photograph showing the electrical connections and jumper boards between the main STM head and the second STM tip is shown in Fig. 2(c). A photograph showing a blow up of a highly oriented pyrolytic graphite (HOPG) sample and two

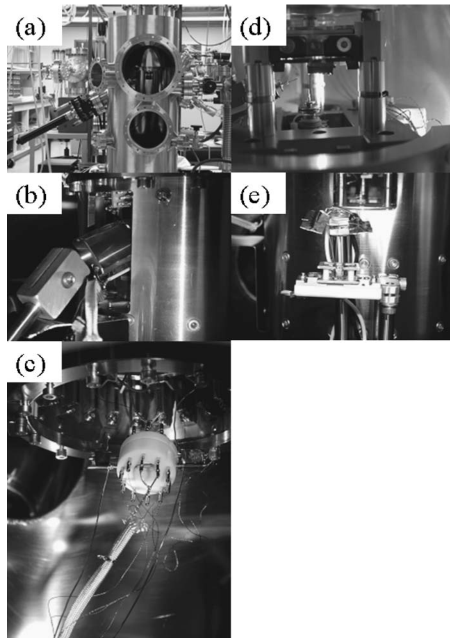

FIG. 2. Photographs of STM system. (a) View of the main section of the STM chamber showing the linear translator holding the second tip. (b) Close-up image of the mechanical arm holding the second STM tip. (c) Close-up image of the electrical connector for the second STM tip. (d) View of STM blown up to show just the sample and the two STM tips. (e) View of the e-beam tip cleaning facility.

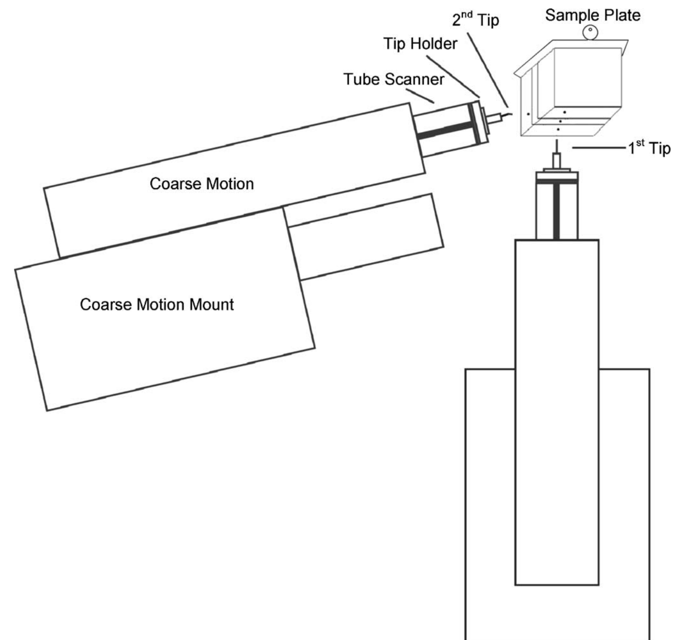

FIG. 3. Schematic diagram of two-tips and sample geometry for the STM head. This is a side view showing the main STM tip comes from the bottom to image the sample, while the second STM tip comes from the left side to image the sample on a perpendicular surface.

STM tips is shown in Fig. 2(d). A close look at this photograph shows the first STM tip pointing straight up toward the sample. Just to the left is the second STM tip. It approaches the sample at angle about 15° off the horizontal. Finally, a photograph showing the electron-beam tip cleaning stage just below the cutout used for tip and sample transfers to the head is shown in Fig. 2(e).

A schematic diagram showing the geometry of the two STM tips and the sample is shown in Fig. 3. The STM sample plate mounts in the standard position on the STM head. The sample is indium soldered to a piece of tantalum sheet metal. One side of the tantalum foil is spot welded to the standard Omicron sample plate, while the other side holds the sample. Two perpendicular surfaces of the sample are exposed to the two STM tips. Once in place the STM sample mount is fixed in position, while the tips are macroscopically positioned in three orthogonal directions. The tips approach their imaging surfaces from a direction almost normal to their imaging surface. The second STM tip can be perpendicular to the sample surface after bending the tip (as illustrated in Fig. 3). In this perpendicular geometry each STM tip can image a separate side surface of the sample yet be positioned directly on the edge of the sample within nanometers of each other.

Getting the tips this close does depend on the radius or geometry at the end of the tip. If one assumes both tips are small spheres of radius R and that they are imaging perpendicular surfaces near the outside corner of the sample it is then possible to use geometry to calculate the straight line distance d through the sample between the two tunneling junctions. To a good approximation $d[R(\mathrm{nm})]=0.5R(\mathrm{nm})+0.5$. For a 2 nm radius tip available commercially, d is equal to 1.5 nm. We typically use single crystal W(111) tips, however. These tips form (111) facets with a single atom on the very end. Here R is closer to 0.1 nm. We do not, however, believe that it is important to have the tips this close. The interesting effects are going to occur as one tip scans further away from the other, and allows us to observe the loss of coherence (e.g., energy, momentum, or spin).

To help communicate how a typical experiment would work, the sample is drawn to be three-dimensional in Fig. 3. On the sample a heterostructure is illustrated using two dark lines. With this system one can inject charge with the second tip into the substrate (note that the tunneling location is shown as a dark dot), then detect that charge in the substrate, in the heterostructure, or in the cap layer with the first tip (again, the three different tunneling locations are shown as three dark dots). This allows the role the interfaces between the different layers plays in the transport process to be studied.

The sample is grounded and each tip is separately biased. This allows us to inject charge with one tip and detect that same charge with the other tip. In addition, the sample grounding wire can be first connected to a picoammeter and then to a dc power supply. These connections allow us to monitor the current to and from ground, control the bias on the sample, or isolate the sample entirely. Our goal is to be able to completely control the source of charge (or spin in the case of ferromagnetic metal tips) injected and detected from the sample. That is, if we inject an electrical current with certain spin polarization using the first STM tip, we want to make sure the same electrons flow to the second STM tip. In addition, when the two tips are only nanometers apart we will be within the ballistic transport region and can study coherent transport between the two coupled tunnel junctions.

C. STM data acquisition and control

Data acquisition and control are accomplished using two sets of commercially available feedback electronics and computer control software. The cabling for each is ran through two sets of electrical feedthroughs mounted on tees at the top of the main STM mounting flange. The acquisition and control programs run on a windows-based computer with boards for both digital-to-analog and analog-to-digital conversions. For macroscopic STM tip positioning, manual control via a remote control box moves a “stick-slip” stage, whereas the computer controls the tube scanner for microscopic positioning. Using an optical camera with zoom it is possible to position the two tips within a few microns of each other. Then, an automated tip approach uses the coarse motion stages to establish tunneling. Once the two tips are tunneling and imaging their particular surface, the next step is to position them adjacent to each other and within a few nanometers. This process involves imaging the surface at the micron scale with both tips. Then, the tip scan area is moved closer to the edge of the sample, just as normally done by people studying cleaved samples with a single tip. Once the edge is reached the image will show a sudden drop off in the topography. If the edge is cleaved sharply then this will appear in the image as a sharp line at which point the topography begins dropping. After the edge is found with both tips on their respective surfaces, then the image is again moved along the edge of the sample until the image of the sample begins to pick up the other tip. At this point, when the two tips are next to each other but on separate surfaces we can be certain that they are only a few nanometers apart.

The program also allows simultaneous acquisition of topographic images and tunneling spectra, as well as real-time display and rapid data reduction. The output files are in a format directly accessible by commercial image processing software packages. Imaging and spectroscopy parameters are modifiable by the user to enable a variety of experiments and to allow for instant modification of scanning parameters upon calibration. The feedback, amplifier, and filter electronics are commercially available.

D. First tip images second tip: Stability and unique current tracking demonstration

An illustration of some of the capabilities of this new system is shown in Fig. 4(a). The image shows a picture of the second STM tip taken by the first STM tip. To collect this data we had the two tips image the same surface as illustrated in Fig. 4(b). The second tip was then taken out of tunneling but left near the surface so no current would flow between the second tip and the sample. The first tip was then set to scan a $10\times 10\ \mu m^2$ area. The second tip was then found in the image area. To confirm that we were imaging the second STM tip and not some other artifact we feed the electrical output current from the second STM tip into the analog-to-digital (A/D) board on the back of the electronics for the first STM tip as also illustrated in Fig. 4(b). We can do this measurement because on the electronics for the first STM tip you can read analog signals while simultaneously imaging with the first tip. The data shown in Fig. 4(a) are the current flowing through the second STM tip from the first tip. Most of the image is white, which represents no current flowing through the second tip (during this part of the image the current flows to ground through the sample). Then, the image turns black when the first STM tip starts to tunnel into the second STM tip (and not into the sample). Black in this case in the set point tunneling current for the first STM tip which was set to 1 nA. Note that the scan direction for the image in Fig. 4(a) is from top to bottom. The feedback circuit for the first STM tip can track up the second STM tip, but once it reaches the top of the curvature of the shaft of the second STM tip the feedback circuit cannot drive the tip down fast enough to complete the image on the bottom side of the tip. This is why the image of the second tip appears curved on the top side but straight on the bottom side.

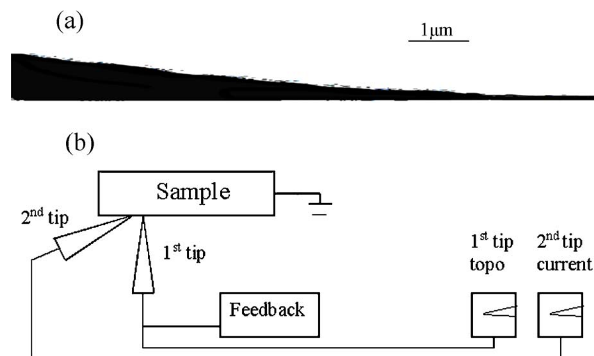

FIG. 4. (a) This image shows a picture of the second STM tip as imaged by the first STM tip. This image is a current image not a topography image. Here the second tip is held stationary and close to the surface. When the first tip tunnels to the second tip the current flowing through the second tip is collected simultaneously by the A/D electronics associated with the first tip (black represents −1 nA and white represents 0 nA). (b) Illustration of the orientation of the sample and both tips when the data were collected for part (a).

E. First tip atomic resolution image using current from second tip

The performance of the first STM tip is demonstrated in Fig. 5. This set of STM images was taken from the thick slab of graphite (HOPG) using a constant current imaging method. The side mounted STM tip (made of polycrystalline tungsten) was set with a negative bias (sample is grounded) and 1 nA of current. This results in the electrons leaving the side mounted tip (second STM tip) and entering the sample. The bottom mounted STM tip (first STM tip, also made of polycrystalline tungsten) was set with a positive bias and 1 nA of current. This results in the electrons leaving the sample and entering the bottom mounted tip. The images were taken with the bottom mounted STM tip while the side mounted STM was held at one position. The sample is at room temperature and the system is under UHV. An image of the HOPG surface that measures $500\times 500\ nm^2$ is shown in Fig. 5(a). Here a step can be seen running diagonally near the top of the image. A higher magnification image of this step is shown in Fig. 5(b). It appears that some contamination decorates the step edge. Finally, an atomic resolution image of the surface is shown in Fig. 5(c). We present these images only to demonstrate that the imaging capability of the bottom

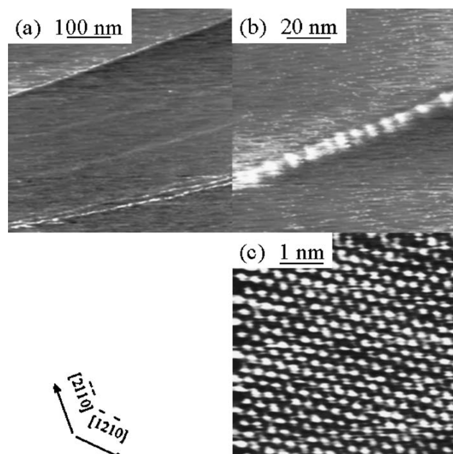

FIG. 5. Data taken with first STM tip using the current supplied by the second tip. Constant current STM images of HOPG using a set point of 1 nA, side tip at a bias of −3 V (injecting electrons) and the underneath tip at +3 V (detecting electrons), and sample is at ground. (a) A 500×500 nm^2 image with a vertical scale of 0.5 nm. (b) A 100×100 nm^2 image with a vertical scale of 0.5 nm. (c) A 5×5 nm^2 image showing atomic resolution.

mounted STM tip (first STM tip) has been maintained after our modifications. In order to show a large and medium scale image on HOPG it was necessary to find something identifiable like the step. These images were taken with the two tips microns apart, not nanometers apart.

F. Second tip image *X-Y* grid: Stability and drift control demonstration

The performance of the second STM tip is demonstrated in Fig. 6. These two STM images were taken from a commercially available calibration sample. This sample is a silicon wafer that has a square grid of square holes etched into the silicon and then coated with platinum (Pt). The square holes are about 0.3 μm wide and are spaced about 1.0 μm apart in both the x and y directions. The depth of the holes is about 0.1 μm. The data were taken using a constant current imaging method. The STM tip (second tip) is also made of Pt and was set to have a negative bias (sample is grounded) and 1 nA of current. The sample is at room temperature and the system is under UHV. The images of the Pt coated Si X-Y grid measure 3×3 μm^2. The two images were taken back-to-back to demonstrate the drift rate and scan reproducibility. The geometry of the holes is modified by the convolution of the tip shape with the hole shape.

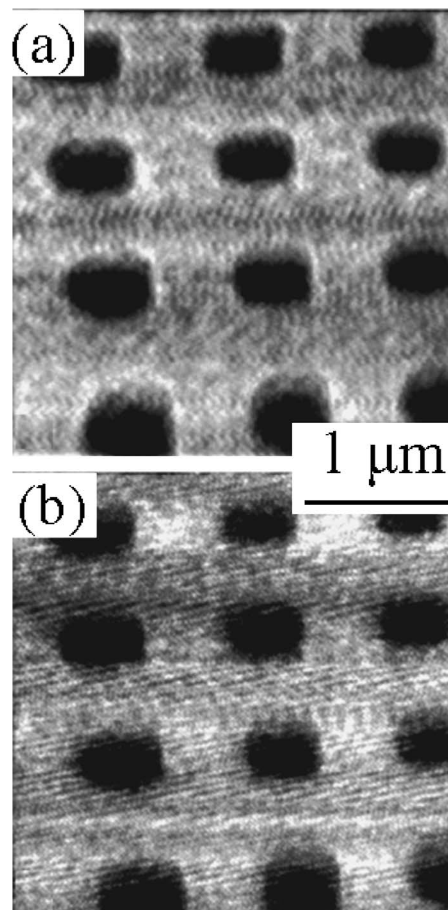

FIG. 6. Data taken with second STM tip. Constant current STM images of a platinum coated silicon wafer with etched X-Y grid of holes. The holes are about 0.3 μm wide and are spaced about 1.0 μm apart. The set point is 1 nA with a tip bias of −3 V (injecting electrons) and the sample is grounded. (a) A 3×3 μm^2 image with a vertical scale of 0.1 μm. (b) The same area and image size as shown in (a) taken sequentially to show the drift rate scan reproducibility.

III. SUMMARY

We have taken a commercial low-temperature STM system and modified it to have two independently controlled STM tips that image perpendicular surfaces. We can inject current with one tip and detect that same current with the second tip. By giving the injected electrons specific properties, either energy, momentum, or spin, for example, we plan to tag these electrons and then see the changes in these tagged electrons after they move through a portion of the sample. Since the two tips are mounted at right angles to each other the scanner components do not interfere with each other. Also, since the two tips image different surfaces their radius of curvatures does not interfere with each other. This allows the two tips to be positioned within a few nanometers of each other. If the sample contains nanostructures, such as flat epilayers or quantum dots, then we can inject charge into the layers and detect them immediately thereafter. As a final bonus, our modifications allow for one to detach the second STM tip, replace the inner copper cup with a new one, and recover the original LT-STM.

ACKNOWLEDGMENTS

The work is supported by the NSF-MRI program under Grant No. DMR-0215872 and NSF-EM program under Grant No. DMR-0405036.

[1] D. Gammon, E. S. Snow, B. V. Shanabrook, D. S. Katzer, and D. Park, Science **273**, 87 (1996).
[2] M. Johnson and R. H. Silsbee, Phys. Rev. Lett. **55**, 1790 (1985).
[3] G. Binnig, H. Rohrer, Ch. Gerber, and E. Weibel, Phys. Rev. Lett. **50**, 120 (1983).
[4] L. D. Bell and W. J. Kaiser, Phys. Rev. Lett. **61**, 2368 (1988).
[5] R. A. Wolkow, Phys. Rev. Lett. **68**, 2636 (1992).
[6] P. M. Thibado, Y. Liang, and D. A. Bonnell, Rev. Sci. Instrum. **65**, 3199 (1994).

[7] J. B. Smathers, D. W. Bullock, Z. Ding, G. J. Salamo, P. M. Thibado, B. Gerace, and W. Wirth, J. Vac. Sci. Technol. B **16**, 3112 (1998).
[8] M. Krause, A. Stollenwerk, C. Awo-Affouda, B. Maclean, and V. P. LaBella, J. Vac. Sci. Technol. B **23**, 1684 (2005).
[9] L. J. Whitman, P. M. Thibado, F. Linker, and J. Patrin, J. Vac. Sci. Technol. B **14**, 1870 (1996).
[10] C. A. Ventrice, V. P. LaBella, and L. J. Schowalter, J. Vac. Sci. Technol. A **15**, 830 (1997).
[11] P. Geng, J. Marquez, L. Geelhaar, J. Platen, C. Setzer, and K. Jacobi, Rev. Sci. Instrum. **71**, 504 (2000).
[12] V. P. LaBella, H. Yang, D. W. Bullock, P. M. Thibado, P. Kratzer, and M. Scheffler, Phys. Rev. Lett. **83**, 2989 (1999).
[13] Z. Ding, D. W. Bullock, P. M. Thibado, V. P. LaBella, and K. Mullen, Phys. Rev. Lett. **90**, 216109 (2003).
[14] S. Tsukamoto, B. Siu, and N. Nakagiri, Rev. Sci. Instrum. **62**, 1767 (1991).
[15] Q. Niu, M. C. Chang, and C. K. Shih, Phys. Rev. B **51**, 5502 (1995).
[16] H. Okamoto and D. Chen, J. Vac. Sci. Technol. A **19**, 1822 (2001).
[17] H. Grube, CB. C. Harrison, J. Jia, and J. J. Boland, Rev. Sci. Instrum. **72**, 4388 (2001).
[18] H. Okamoto and D. Chen, Rev. Sci. Instrum. **72**, 4398 (2001).
[19] S. Hasegawa and F. Grey, Surf. Sci. **500**, 84 (2002).
[20] X. Lin, X.-B. He, J.-L. Lu, G. Li, Q. Huan, D. X. Shi, and H. J. Gao, Chin. Phys. **14**, 1536 (2005).
[21] A. J. Melmed, J. Vac. Sci. Technol. B **9**, 550 (1991).
[22] Z. Zheng, Y. Qi, D. Y. Xing, and J. Dong, Phys. Rev. B **59**, 14505 (1999).
[23] K. Xia, P. J. Kelly, G. E. W. Bauer, A. Brataas, and I. Turek, Phys. Rev. B **65**, 220401(R) (2002).